REGULAR ARTICLE

blood advances

Activation priming and cytokine polyfunctionality modulate the enhanced functionality of low-affinity CD19 CAR T cells

Ilaria M. Michelozzi,[1] Eduardo Gomez-Castaneda,[1,*] Ruben V. C. Pohle,[1,*] Ferran Cardoso Rodriguez,[2] Jahangir Sufi,[2] Pau Puigdevall Costa,[3] Meera Subramaniyam,[1] Efstratios Kirtsios,[1] Ayad Eddaoudi,[4] Si Wei Wu,[1] Aleks Guvenel,[1] Jonathan Fisher,[5] Sara Ghorashian,[5] Martin A. Pule,[6] Christopher J. Tape,[2] Sergi Castellano,[3,7,†] Persis J. Amrolia,[1,8,†] and Alice Giustacchini[1]

[1]Molecular and Cellular Immunology Section, UCL Great Ormond Street Institute of Child Health, London, United Kingdom; [2]Cell Communication Lab, Department of Oncology, University College London Cancer Institute, London, United Kingdom; [3]Genetics and Genomic Medicine Department, Great Ormond Street Institute of Child Health, University College London, London, United Kingdom; [4]Flow Cytometry Core Facility and [5]Developmental Biology and Cancer Section, UCL Great Ormond Street Institute of Child Health, London, United Kingdom; [6]Cancer Institute, University College London, London, United Kingdom; [7]UCL Genomics, Zayed Centre for Research into Rare Disease in Children, University College London, London, United Kingdom; [8]Department of Bone Marrow Transplant, Great Ormond Street Hospital for Children, London, United Kingdom

Key Points

- Low-affinity CAT CAR T cells are characterized by a unique pattern of activation priming and cytokine polyfunctionality.
- The enhanced functionality of low-affinity CAT CAR T cells is a consequence of an antigen-dependent priming.

We recently described a low-affinity second-generation CD19 chimeric antigen receptor (CAR) CAT that showed enhanced expansion, cytotoxicity, and antitumor efficacy compared with the high-affinity (FMC63-based) CAR used in tisagenlecleucel, in preclinical models. Furthermore, CAT demonstrated an excellent toxicity profile, enhanced in vivo expansion, and long-term persistence in a phase 1 clinical study. To understand the molecular mechanisms behind these properties of CAT CAR T cells, we performed a systematic in vitro characterization of the transcriptomic (RNA sequencing) and protein (cytometry by time of flight) changes occurring in T cells expressing low-affinity vs high-affinity CD19 CARs following stimulation with CD19-expressing cells. Our results show that CAT CAR T cells exhibit enhanced activation to CD19 stimulation and a distinct transcriptomic and protein profile, with increased activation and cytokine polyfunctionality compared with FMC63 CAR T cells. We demonstrate that the enhanced functionality of low-affinity CAT CAR T cells is a consequence of an antigen-dependent priming induced by residual CD19-expressing B cells present in the manufacture.

Introduction

T cells that are genetically engineered to express CD19 chimeric antigen receptors (CAR T cells) have shown remarkable efficacy in relapsed/refractory (r/r) B-cell malignancies, leading to clinical licensing for use in r/r B-cell acute lymphoblastic leukemia (B-ALL) and non-Hodgkin lymphoma.[1] Despite this success, several safety and efficacy hurdles remain.[2] CAR T cells can trigger potent immune responses leading to transient but potentially life-threatening inflammatory events, such as cytokine release syndrome and neurotoxicity.[3,4] Thus, the design of versatile CAR T cells, capable of balancing safety and efficacy, is contingent on our understanding of the molecular mechanisms underlying CAR T-cell

Submitted 5 July 2022; accepted 9 November 2022; prepublished online on *Blood Advances* First Edition 1 December 2022; final version published online 27 April 2023. https://doi.org/10.1182/bloodadvances.2022008490.

*E.G.-C. and R.V.C.P. contributed equally to this study.

†S.C. and P.J.A. contributed equally to this study.

The RNA sequencing (RNA-seq) data and analyses are available at NCBI's Gene Expression Omnibus (GEO) data repository with the accession code GSE157584. Mass cytometry raw and processed data will be made publicly available at the Cytobank Community Server (accession number 1481, https://community.cytobank.org).

Data are available on request from the corresponding author, Alice Giustacchini (a.giustacchini@ucl.ac.uk).

The full-text version of this article contains a data supplement.

function. The engagement of CARs to their cognate antigens results in the activation of CAR T cells and promotes their rapid expansion as well as their differentiation into distinct T-cell subsets, mediating tumor cytolysis (effector cells) and providing long-lasting protection (memory cells). Because tumor cell recognition by CAR T cells relies on the binding of the CAR's single-chain variable fragment (scFv) to its epitope, fine tuning the affinity of CARs to their antigens has become a strategy to modulate the strength of CAR T-cell responses.[5]

The affinity of CARs is determined by their binding kinetics and the rates at which they associate to and dissociate from their targets. The optimal affinity of a CAR is likely to vary depending on a number of factors, including the CAR design, the CAR expression levels, and the antigen density on the target cells.[6,7] Chimeric immunoreceptors have an activation ceiling above which increasing the binding affinity does not improve T-cell activation but can rather result in T-cell exhaustion.[8] In contrast, by reducing CAR scFv affinity, the strength of the T-cell signal can be modulated, so that CAR T cells discriminate different levels of antigen expression. CARs exhibiting slower antigen-association rates to ErbB2, EGFR, and CD123 targets showed reduced activation in response to low antigen concentrations, favoring differential targeting of tumor cells overexpressing the target vs normal tissue expressing the same target at physiological levels.[8-10] We have recently described a novel low-affinity CD19 CAR (CAT), with epitope, structure, and stability similar to the widely used FMC63, but characterized by faster rates of antigen dissociation, leading to an overall 40-fold reduction of its affinity.[11] Preclinical testing of CAT CAR T cells has revealed greater antigen-specific cytotoxicity, higher proliferation both in vitro and in vivo, and more potent in vivo antitumor activity when compared with FMC63. In a phase 1 clinical trial in patients with high-risk treatment-refractory pediatric B-ALL, CAT CAR T cells resulted in lower toxicity in terms of severe cytokine release syndrome and displayed greater expansion than that reported for the FMC63-based tisagenlecleucel, as well as excellent persistence.[11] These results were recently confirmed in a multicenter phase 1 trial in r/r adult B-ALL.[12]

The molecular mechanisms through which the fine tuning of CARs affinity influences CAR T-cell phenotypes and functions are largely unknown. The interaction between T-cell receptor (TCR) and the peptide-major histocompatibility complex (MHC), however, offers some insight into how immunoreceptors' affinity can dramatically influence T-cell function.[13] Faster target off-rates in TCRs allow a single peptide-MHC to serially trigger several TCRs, resulting in amplified and sustained T-cell activation.[13] Similar to TCRs, low-affinity CARs may lead to enhanced T-cell activation and decreased exhaustion.

Herein, we performed a systematic in vitro characterization of the molecular and biochemical changes occurring in CAR T cells, comparing a low-affinity CD19 CAR (CAT) with a high-affinity one (FMC63). By combining bulk RNA-seq with single-cell mass cytometry analyses (cytometry by time of flight [CyTOF]), we show that the expression of the CAT CAR induces an antigen-dependent priming in response to low concentrations of CD19-expressing B cells found in the manufactured product. Upon antigen stimulation, we identified distinct molecular features downstream of CAT CAR activation responsible for enhancing CAT CAR T-cell responses.

Methods

Ex vivo T-cell expansion

Freshly isolated peripheral blood mononuclear cells (PBMCs) and CD19-depleted PBMCs were cultured in TexMACS medium (Miltenyi Biotec, Bergisch Gladbach, Germany), an optimized T-cell medium. To induce T-cell expansion, CD3/CD28 beads (CTS Dynabeads CD3/CD28, Thermo Fisher Scientific) were added to cells in MACS GMP cell differentiation bags (Miltenyi Biotec) at a 1:3 lymphocyte:bead ratio. CD3/CD28 beads were magnetically removed from the culture on day 5 and CAR T cells rested for 48 hours before proceeding to antigen stimulation.

Lentiviral vector transduction

Following overnight activation with CD3/CD28 beads, 0.5×10^6 bead-activated T cells were suspended in 0.5 mL of TexMACS, transduced to express CD19 CAR construct (FMC63 or CAT) with 1 mL of lentiviral (LV) supernatant in RetroNectin-coated (Takara Bio, Kusatsu, Shiga, Japan) 24-well plates and spinoculated at 1000*g* for 40 minutes at room temperature. Generally, 2×10^6 to10×10^6 bead-activated T cells per donor per construct were seeded for transduction.

CAR T-cell cocultures

Briefly, bead-activated T cells were incubated for 48 hours in optimized T-cell medium before stimulation. Untransduced (UNTR), FMC63, or CAT bead-activated T cells (0.1×10^6) were seeded in 96-well plates in complete TexMACS medium in a 1:1 ratio with irradiated (40 Gy) NALM6. Generally, 0.1×10^6 to 6×10^6 bead-activated T cells per donor per condition (UNTR, FMC63, or CAT) were stimulated.

Unstimulated, bead-activated T cells per donor, condition, and time point were kept in culture under the same experimental conditions.

Flow cytometry fluorescence-activated cell sorting (FACS) and antibody staining

All flow cytometry FACS experiments included fluorescence minus one and single antibody–stained BD CompBeads (BD Biosciences) controls to set expression the threshold and to calculate compensation, respectively. Experiments were performed on a cell sorter FACSAria III (BD Biosciences) and on a CytoFLEX analyzer (Beckman Coulter Inc, Brea, CA) and analyzed with FlowJo software version 10.6.1 (BD Biosciences) and Cytobank platform (www.cytobank.org). Details on the antibody panels can be found in the supplemental Methods.

Mass cytometry analysis

After 24 hours of stimulation, samples in all experimental conditions were treated with Brefeldin A (BioLegend) (1:1000) at 37°C for 4 hours to favor intracellular cytokine accumulation and were then fixed with 1.6% formaldehyde for 10 minutes at room temperature. Fixed samples were processed, barcoded (Cell-ID 20-Plex Pd Barcoding Kit, Fluidigm), and stained, as previously described.[14] Two independent mass cytometry experiments were performed

and the antibodies used are listed in supplemental Table 3. The samples were analyzed on a Helios mass cytometer (Fluidigm). EQ Four Element Calibration Beads (Fluidigm) were added to cell suspensions immediately before acquisition to guarantee inter-sample comparability.

Statistical analyses

Data are shown as mean ± standard error of the mean and statistical analyses were performed in R calculating paired-samples *t* tests across experimental conditions, unless otherwise stated.

Earth mover's distance (EMD)–related statistical analyses between selected experimental conditions, and the results of polyfunctionality analysis are reported in supplemental Table 5.

Results

Generation and quality assessments of low- and high-affinity CD19 CARs from healthy donors

To dissect the molecular mechanisms behind the functional differences observed between low- and high-affinity (CAT and FMC63, respectively) CD19 CAR T cells,[11] we interrogated the transcriptional and protein expression profiles of T cells LV transduced with CARs differing only in their scFv (supplemental Figure 1A). We performed bulk transcriptomic analyses (RNA-seq) to identify CAR T-cell distinct gene expression signatures and mass cytometry analyses (CyTOF) to model differences in their downstream signaling at a single-cell resolution.[14] RNA-seq and CyTOF readouts from UNTR controls and T cells LV transduced to express CAT or FMC63 CD19 CARs from healthy donors (HD1-HD27, supplemental Table 1) were compared at baseline and after stimulation with $CD19^+$ ALL cell line NALM6 (unstimulated and stimulated conditions, respectively), as schematized in Figure 1A. We ruled out significant differences in the transduction of the 2 CARs by FACS, assessing the percentage of $mCherry^+$ T cells (lentivirus fluorescent reporter) across donors and experimental conditions. These ranged between 11.50% and 93.80% (median, 39.1%) in FMC63 and 13.40% to 93.60% (median, 36.25%) in CAT (Figure 1B, left) and were thus comparable among individual HDs. In agreement, we found similar transgene expression levels between the 2 CARs by measuring mCherry mean fluorescent intensity, a proxy for CARs expression (Figure 1B, right) and by quantifying CARs surface expression levels (Figure 1C) and number of integrated vector copies (supplemental Figure 1B). Finally, we assessed CAT and FMC63 CAR T-cell products for their CD4:CD8 ratios and memory T-cell subset composition, because these characteristics can both affect CAR T-cell persistence and antitumor activity.[15,16] Although no difference in CD4:CD8 ratios was observed in the absence of antigen stimulation (Figure 1D), the proportion of memory subsets differed in unstimulated FMC63 and CAT CAR T cells, as measured by FACS at 10 days after transduction. CAT CAR T cells exhibited a significant increase in the fraction of central memory T cells (T_{CM}, $CD62^+CD45RA^-$) as compared with both UNTR and FMC63 conditions (Figure 1E, left). The increase in T_{CM} was largely at the expense of T effector memory cells (T_{EM}, $CD62^-CD45RA^-$) and effector memory re-expressing CD45RA (T_{EMRA}, $CD62^-CD45RA^+$), whose proportion was significantly reduced in CAT vs FMC63 CAR T cells and in both CARs as compared with UNTR control (Figure 1E, middle and right). These assessments confirmed that our CAR T-cell products were suitable to investigate the molecular features of CAT and FMC63 CAR T cells.

Low-affinity CD19 CAT CARs display higher activation priming during CAR T-cell manufacture

Next, we performed bulk RNA-seq of FACS-sorted UNTR T cells ($CD3^+$) and FMC63 or CAT CAR T cells ($CD3^+mCherry^+$) with or without a 24-hour stimulation with NALM6. Transcriptomics confirmed that mCherry was an accurate proxy for CAR transgene expression levels, as evidenced by the significant positive correlation between the mean fluorescent intensity of mCherry by FACS and the normalized RNA-seq counts aligning to the scFv region of each of the 2 CARs (supplemental Figure 2A). Similarly, the proportion of CD4 and CD8 T cells detected by FACS was in line with the *CD4* and *CD8* messenger RNA levels (supplemental Figure 2B-C). Principal component analysis (PCA) of the 500 most variable expressed genes (top 100 genes shown in supplemental Figure 2D), distributed samples according to a T-cell activation gradient (PC1, from UNTR to CAR-activated samples) (Figure 2A). The majority of variance in gene expression across experimental conditions was explained by CD19-mediated CAR activation. As expected, UNTR T cells not expressing any CARs were largely unaffected by antigen stimulation (Figure 2A). Similarly, PCA on protein expression from CyTOF, based on EMD scores (a sensitive measure of multivariate changes in protein levels),[17] under the same experimental conditions and timepoints than the gene expression, followed a similar gradient of sample activation, shifting from UNTR samples to antigen-stimulated CAR T cells on PC1 (Figure 2B; supplemental Figure 3A). The most variable genes upregulated upon stimulation with NALM6 in both FMC63 and CAT CAR T cells included genes involved in T-cell activation (*IL2RA*, *GZMB*) and proliferation (*PCNA*, *LDHA*), which are expressed at very low levels in control T cells (supplemental Figure 2D). Consistent with this, the highest protein expression variation was from markers of T-cell activation (CD25, NFAT1, HLA-DR) and proliferation (pRB) (supplemental Figure 3A). In both RNA and protein analyses, unstimulated CAR T cells had an intermediate RNA/protein expression profile between UNTR and stimulated CAR T cells. This suggests that CAR expression on its own, in the absence of antigen stimulation, induces basal T-cell activation (Figure 2A-B).

To gain further insights into the intermediate activation state observed in unstimulated CAR T cells, we fuzzy clustered individual samples by their gene expression to resolve intermediate cell states and trajectories (Figure 2C).[18] We identified 2 clusters, highly enriched for either inactive T cells (cluster 1, which includes UNTR samples) or antigen-activated CAR T cells (cluster 2, which includes stimulated CAR T samples) (Figure 2C). Notably, the probability of unstimulated CAT samples belonging to cluster 2 (activated CAR T cells) was substantially higher than that of unstimulated FMC63 (4/6 HDs in CAT vs 0/6 HDs in FMC63), further evidencing the functional proximity between unstimulated CAT and activated CAR T cells. Using gene-set enrichment analysis on the Hallmark collection, we confirmed that although antigen stimulated CAT and FMC63 CAR T cells have similar enrichment for most of the gene sets involved in immune functions and cell proliferation, CAT CAR T cells are uniquely enriched for T-cell

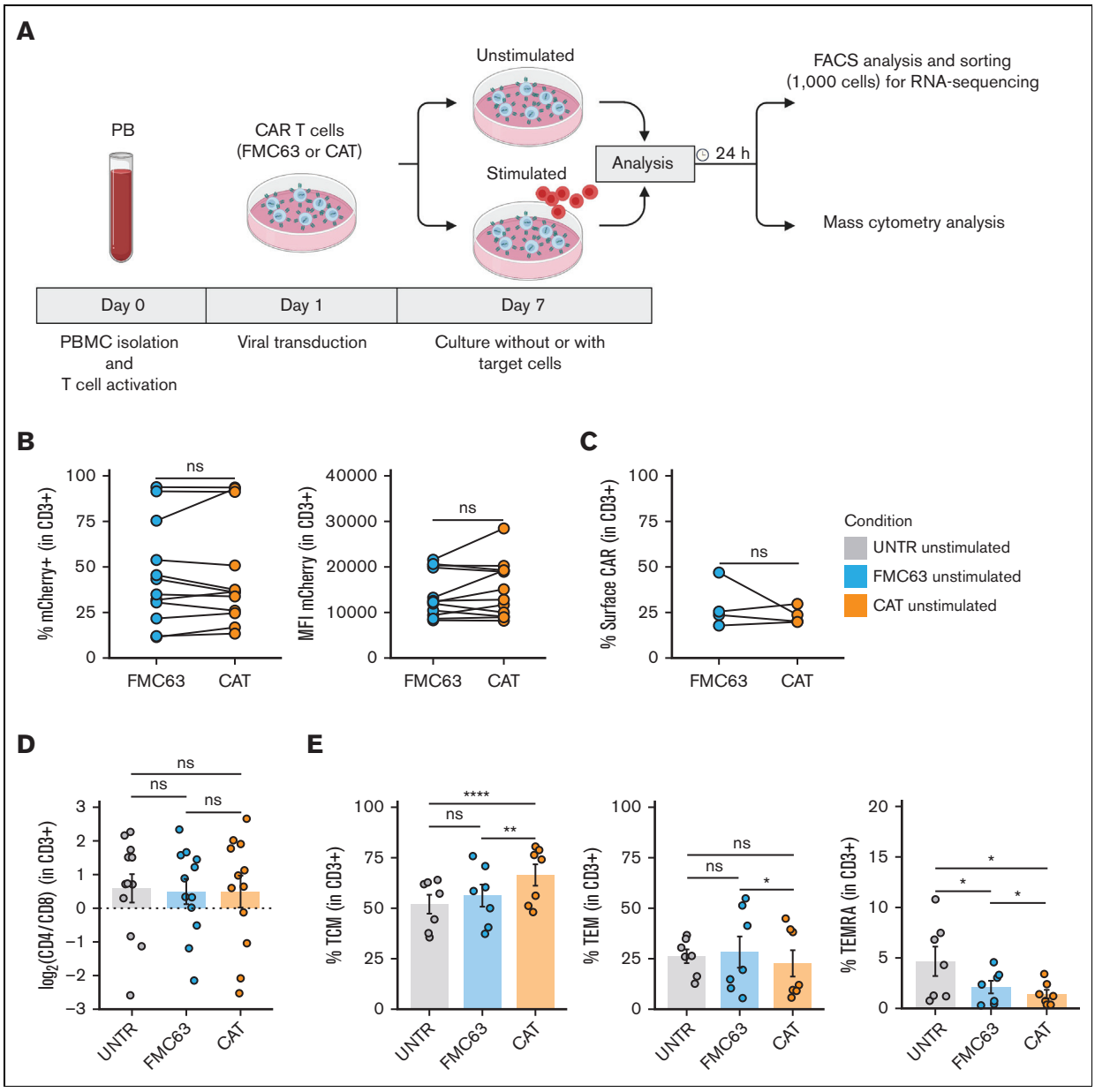

Figure 1. Generation and phenotypic characterization of CAR T cells from HD-PBMCs. (A) Experimental workflow. PBMCs were isolated from HDs and LV transduced to express CD19 CAR construct (FMC63 or CAT) following overnight activation with CD3/CD28 beads. Six days after transduction, CAR T cells were cultured without (unstimulated) or with target cells (NALM6) at a 1:1 ratio (stimulated). Unstimulated and stimulated cells were analyzed by flow cytometry and sorted for RNA-seq 24 hours poststimulation. Mass cytometry analysis was performed on unstimulated and stimulated cells 24 hours poststimulation. Activated UNTR T cells were used as a control throughout the experiment. (B) (Left) spaghetti plots showing transduction levels of CAR T cells as percentage of mCherry$^+$ (in CD3$^+$) and (right) as MFI of mCherry in unstimulated transduced T cells measured by FACS 7 days posttransduction. Lines connect results from individual donors (n = 12 HDs, n = 3 independent experiments). (C) Spaghetti plot showing the percentage of surface CAR expression (in CD3$^+$) in unstimulated transduced T cells measured by FACS 10 days posttransduction. Lines connect results from individual donors (n = 4 HDs, n = 1 independent experiment). (D) Variation (log2 fold change) of CD4 and CD8 proportion in unstimulated UNTR T cells and FMC63 and CAT CAR T cells measured by FACS 7 days posttransduction. The dotted horizontal line (0) represents the conditions in which CD4 = CD8. Data represent mean ± SEM (n = 12 HDs, n = 3 independent experiments). (E) Bar plots showing the percentage of T_{CM} (CD45RA$^-$CD62L$^+$) (left), T_{EM} (CD45RA$^-$CD62L$^-$) (middle), and T_{EMRA} (CD45RA$^+$CD62L$^-$) (right) in unstimulated CD3$^+$ UNTR T cells and FMC63 and CAT CAR T cells measured by FACS 10 days posttransduction. Data represent mean ± SEM (n = 7 HDs, n = 2 independent experiments). (B-E) Statistical significance was calculated by paired *t* test; *$P < .05$, **$P < .01$, and ****$P < .0001$. Each experimental condition is indicated by a specific color code (UNTR, light gray; FMC63, light blue; CAT, orange). MFI, mean fluorescent intensity; SEM, standard error of the mean.

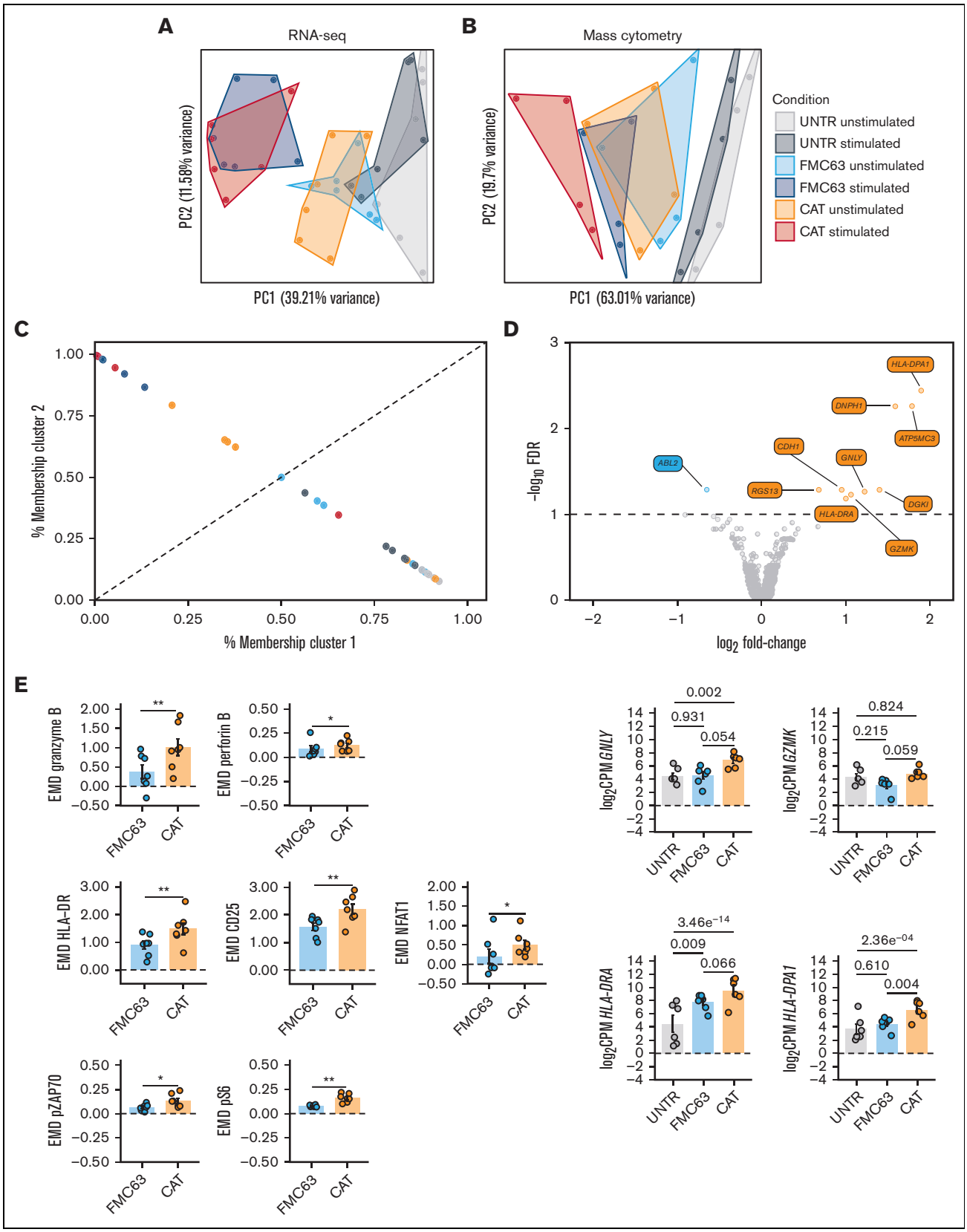

Figure 2. RNA-seq and mass cytometry analyses of unstimulated UNTR and CAR-transduced T cells. (A) PCA of the top 500 variable genes from RNA-seq analysis across all experimental conditions (n = 6 HDs, n = 2 independent experiments). (B) PCA of mass cytometry EMD scores computed at 24 hours poststimulation in $CD3^+$ cells

activation pathways in the absence of antigen stimulation (supplemental Figure 3B).

Next, we compared the transcriptome of FMC63 and CAT CAR T cells, in absence of antigen stimulation. After differential gene expression analysis, we found that only 10 genes were significantly differentially expressed between these 2 conditions (false discovery rate <0.1, supplemental Table 2), 9 of which were upregulated in CAT vs FMC63 CAR T cells. Among those, we found genes involved in cytotoxicity (*GNLY*, *GZMK*) and markers of T-cell activation such as MHC class II molecules (*HLA-DRA* and *HLA-DPA*) (Figure 2D). This supports our previous observation of gene expression in unstimulated CAT resembling more that of antigen-activated CAR T cells than gene expression in unstimulated FMC63 (Figure 2C). Mass cytometry analyses using a panel of antibodies against markers of T-cell activation (supplemental Table 3), confirmed that although unstimulated FMC63 and CAT CAR T cells have similar EMD scores for many of the proteins investigated (supplemental Table 5A), unstimulated CAT CAR T cells have significantly stronger activation priming with higher expression of markers of T-cell activation (HLA-DR, CD25, and NFAT1), proinflammatory (granzyme B, perforin B) and stimulatory/activation-related (granulocyte-macrophage colony-stimulating factor, interleukin 17A [IL-17A]) cytokines, and increased phosphorylation of the TCR/CAR CD3ζ chain (pZAP70) and MTOR downstream effector (pS6) (Figure 2E; supplemental Figure 3C).

Altogether, these results show that unstimulated CAT CAR T cells, before antigenic stimulation, have more pronounced T-cell activation priming than FMC63 CAR T cells.

CD19 stimulation of low-affinity CAT CAR T cells results in a distinct transcriptomic and protein profile with increased activation/proliferation over high-affinity FMC63 CAR T cells

Although antigen-independent CAR activation, also known as tonic signaling, has often been associated with CAR T-cell accelerated differentiation and exhaustion,[19-21] recent data show that the induction of CAR T-cell priming can lead to CAR T enhanced antitumor functions in vivo.[22,23] We wanted to assess the molecular effect of the "activation priming" observed in CAT CAR T cells on their molecular response to antigen stimulation. As the superior cytotoxicity of CAT CAR T cells over FMC63 CAR T cells has previously been shown in functional assays,[11] we focused on characterizing their distinct molecular profiles on exposure to antigenic stimulation. Upon stimulation, we found a slight but statistically significant reduction of the CD4:CD8 ratio in CAT as compared with FMC63 (Figure 3A), largely attributable to a relative decrease of the $CD8^+$ fraction (and increase of $CD4^+$) in FMC63 CAR T cells (supplemental Figure 4A). Interestingly, when looking at the memory T-cell subset composition, we found that CAT CAR T cells continued to exhibit a higher proportion of T_{CM} as compared with FMC63 (Figure 3B), whereas no differences were observed in the expression of exhaustion markers (PD1, TIM3, and LAG3) between the 2 CAR constructs (Figure 3C).

Importantly, the stronger basal activation observed in CAT CAR T cells did not prevent an even stronger molecular response when exposed to CD19-expressing NALM6, as shown by the increase in the expression of proliferation and cytotoxic/stimulatory markers, relatively to the unstimulated constructs (supplemental Figures 5 and 6). Consistent with this, we identified 51 differentially expressed genes, 35 of which were upregulated in CAT compared with FMC63 (Figure 3D; supplemental Table 4). CD19 stimulation in CAT CAR T cells also led to significantly augmented expression of immune stimulatory/proliferation cytokines (*IFNG, CSF2, CXCL8*), and interferon gamma (IFN-γ)-responsive genes (*CIITA*) (Figure 3D; supplemental Figure 4B). Conversely, CAT CAR T cells displayed significantly decreased expression of the genes encoding for CRIF1 (*GADD45GIP1*), an inhibitor of cell cycle progression, and for FOXP3, the Treg-associated transcription factor known to only be transiently expressed in the initial stages of Th1 response and rapidly downregulated afterward[24,25] (Figure 3D). These results suggest that following antigenic stimulation CAT CAR T cells show a different transcriptomic profile resulting in stronger activation and proliferation than stimulated FMC63. In addition, CAT CAR T cells showed increased expression of the *TNFSF4* gene (Figure 3D), encoding for the ligand of the T-cell costimulatory receptor OX40 (OX40L). Although OX40L is mainly expressed by antigen presenting cells to promote T-cell activation, it is also expressed in activating T cells, in which it leads to a homotypic OX40L-OX40 signaling axis promoting T-cell longevity and memory differentiation.[26] Furthermore, we also noted the increased expression of the chemoattractants *CCL4* and *CCL3L1* and genes involved in cell migration (*FLT1*, *DOCK5*) and focal adhesion (*COL6A3*) in stimulated CAT CAR T cells (supplemental Figure 4B).

These observations were further substantiated at the protein level. CAT CAR T cells exhibited a marked increase in the expression (as measured by EMD score) of markers of T-cell activation (CD25) (Figure 3E). Moreover, the augmented gene expression of the MHC class II molecules transactivator CIITA observed in CAT, resulted in a corresponding increase of HLA-DR protein (Figure 3E).[27,28] When measuring the CAR T-cell intracellular signaling, CAT CAR T cells showed enhanced phosphorylation of the effectors of the TCR/CAR CD3ζ chain (pZAP70, pp38) and

Figure 2 (continued) across all experimental conditions (n = 4 HDs, n = 1 independent experiment). (C) Fuzzy clustering analysis of RNA-seq data across all experimental conditions (n = 6 HDs, n = 2 independent experiments). (D) Volcano plot showing differentially expressed genes between unstimulated FMC63 and CAT CAR T cells (top). The dashed horizontal line represents the statistical significance threshold (FDR <0.1). The bar plots show the expression of selected differentially expressed genes (FDR <0.1) in unstimulated UNTR and transduced T cells (bottom). Data represent mean ± SEM (n = 6 HDs, n = 2 independent experiments). (E) Bar plots showing the expression of mass cytometry EMD scores for granzyme B, perforin B, HLA-DR, CD25, NFAT1, pZAP70, and pS6 in unstimulated CAR T cells at 24 hours upon stimulation. The data shown are normalized to stimulated $CD3^+$ UNTR T cells. The dotted horizontal line (0) represents the expression of a specific marker in unstimulated $CD3^+$ UNTR T cells. Data represent mean ± SEM (n = 7 HDs, n = 2 independent experiments). Statistical significance was calculated by paired *t* test; $^*P < .05$ and $^{**}P < .01$. (A-E) Each experimental condition is indicated by a specific color code (unstimulated conditions: UNTR, light gray; FMC63, light blue; and CAT, orange; stimulated conditions: UNTR, gray; FMC63, blue; and CAT, red). FDR, false discovery rate; SEM, standard error of the mean.

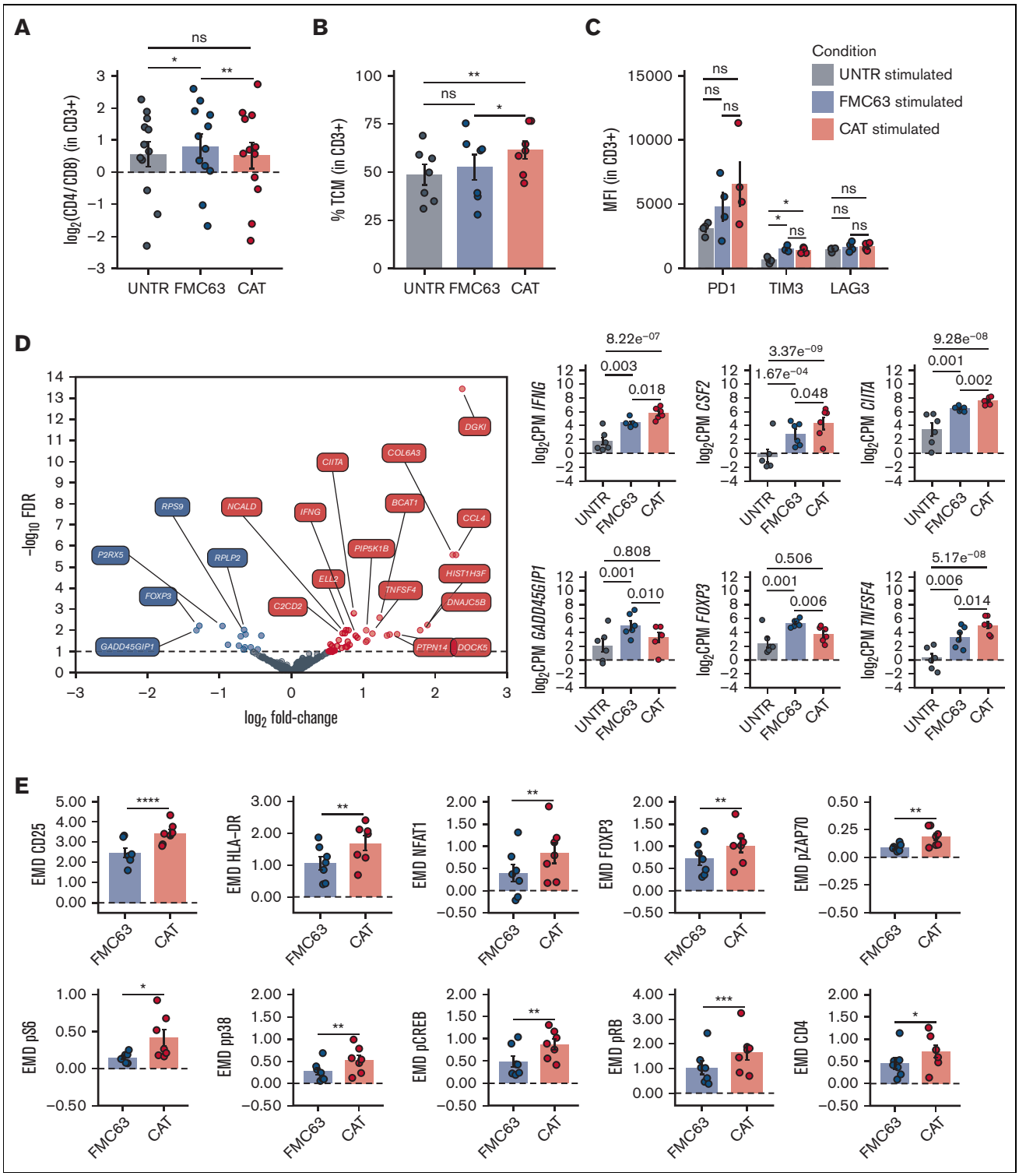

Figure 3. Phenotypic and molecular characterization of stimulated CAR-transduced T cells. (A) Variation (log2 fold change) of CD4 and CD8 proportion in stimulated UNTR T cells and FMC63 and CAT CAR T cells measured by FACS (n = 12 HDs, n = 3 independent experiments). The dotted horizontal line (0) represents the conditions in which CD4 = CD8. (B) Bar plot showing the percentage of T_{CM} ($CD45RA^{-}CD62L^{+}$) in stimulated $CD3^{+}$ UNTR T cells and FMC63 and CAT CAR T cells measured by FACS 96 hours postantigen stimulation (n = 7 HDs, n = 2 independent experiments). (C) Bar plots showing the expression of T-cell exhaustion markers (PD1, TIM3, and LAG3) as MFI in stimulated $CD3^{+}$ UNTR T cells and FMC63 and CAT CAR T cells measured by FACS 96 hours postantigen stimulation (n = 4 HDs, n = 1 independent experiment). (D) Volcano plot showing differentially expressed genes between FMC63 and CAT CAR T cells upon NALM6 coculture (left). The dashed horizontal line represents the statistical significance threshold (FDR <0.1). Bar plots showing the expression of selected differentially expressed genes (FDR <0.1) in stimulated UNTR T cells and in CAR T

increased expression of their downstream transcription factors (NFAT1, pCREB, FOXP3). CAT CAR T cells also exhibited significant upregulation of the Target of Rapamycin Complex 1 (mTORC1) downstream effectors (pS6 and pRB), both involved in cell proliferation and protein translation, in line with the previously reported CAT CAR T cells increased proliferative capacity over FMC63.[11]

Our analysis shows that the increased activation priming observed in CAT CAR T cells over FMC63 resulted in an even stronger T-cell activation gene expression and signaling profile when CAT CAR T cells were exposed to antigenic stimulation. These observations are in line with the CAT CAR T cells enhanced cytotoxic functional properties previously reported.[11]

The enhanced functionality of low-affinity CD19 CAR T cells is associated with cytokine polyfunctionality upon antigen stimulation

Next, we assessed CAR T-cell functional phenotypes by measuring intracellular cytokine levels in individual cells by mass cytometry. The overall protein intensities measured by EMD scores indicated an increased expression of effector cytokines (granzyme B, IFN-γ, and tumor necrosis factor α) and of immune stimulatory molecules (granulocyte-macrophage colony-stimulating factor and IL-2) in CAT CAR T cells as compared with FMC63 (Figure 4A). No upregulation was observed for Th2/immune-modulatory cytokines (IL-4, IL-5, and transforming growth factor ß) and for perforin B (supplemental Table 5B).

Next, we investigated the pattern of cytokine coexpression in CAT and FMC63 CAR T-cell responses. The ability of a single T cell to express simultaneously >1 cytokine (polyfunctionality) has been linked to productive immune responses[29,30] and, more recently, described as a distinctive feature of CAR T cells associated with their potency and antitumor efficacy.[31-33] We measured the frequency at which the 8 cytokines included in our analysis were coexpressed in single CAR T cells, thus providing a comprehensive profile of their cytokine polyfunctionality. Upon stimulation with NALM6, 15.02% of FMC63 and 29.60% of CAT CAR T cells were polyfunctional (expressing ≥2 cytokines per cell) (supplemental Table 5N).

Not only the frequency of polyfunctional CAR T cells but also the number of cytokines coexpressed was higher in CAT than in FMC63, with a statistically significant increase in their mean polyfunctionality (Figure 4B) and a marked increment in the proportion of cells expressing combinations of ≥3 cytokines (2.28% in FMC63 vs 7.89% in CAT) (Figure 4C; supplemental Table 5O). The polyfunctional profiles of stimulated CAT CAR T-cell products were dominated by combinations of cytokines involving the effector molecules IFN- γ, tumor necrosis factor α, IL-2, and granzyme B (Figure 4D).

Low-affinity CD19 CAT CAR activation priming is associated with, and driven by, residual CD19-expressing B cells

To investigate whether the mechanism behind the activation priming observed in unstimulated CAT CAR T cells was antigen dependent or independent, we checked whether residual $CD19^+$ B lymphocytes were detectable in the CAR T-cell product and could serve as a potential source of antigen-specific activation.

We monitored the proportion of $CD19^+$ B lymphocytes in culture at different time points. Although B cells were detectable at day 0 in all samples (5.96% of cells on average), at day 8 (5-day stimulation with CD3/CD28 beads, + 3 days rest) they could only be detected in the UNTR condition (2.33% of cells on average), and had completely been depleted from both CAR constructs, as shown by FlowSOM analysis of mass cytometry data, clustering single cells by cell types,[34] and the relative frequencies (Figure 5A; supplemental Figure 7A). Next, we applied the experimental setup described in Figure 1A but including, as an additional experimental condition, CAR T cells generated from CD19-depleted PBMCs. We confirmed effective CD19 depletion by flow cytometry, with an average of 0.041% residual B cells on depletion as compared with 5.96% with the standard protocol (supplemental Figure 7B). The transduction levels obtained in the CD19-depleted CAT and FMC63 CAR T cells were comparable based on the expression of the fluorescent reporter (mCherry) and the vector copies (supplemental Figure 7C-D). The baseline CD4:CD8 ratios only showed a slight increase in CAT as compared with FMC63 CAR T cells (supplemental Figure 7E). Of note, CD19 depletion affected the T-memory subset composition, with CAT CAR T cells no longer displaying any statistical difference when compared with the UNTR control, whereas FMC63 CAR T cells still showed a significant increase in the proportion of T_{EM} when compared with the UNTR control (Figure 5B).

Mass cytometry analyses revealed that the residual B cells in the CAR T-cell manufacture were responsible for the activation priming observed in unstimulated CAT and FMC63 CAR T cells (supplemental Figures 8 and 9). Although CD19 depletion led to a general decrease in the activation priming previously observed in unstimulated CAR T cells, this reduction was more pronounced in CAT (supplemental Figure 8) than in FMC63 (supplemental Figure 9). Therefore, upon B-cell depletion we no longer detected statistically significant differences between CAT and FMC63 in the expression of T-cell activation markers (HLA-DR, CD25, and NFAT1), proinflammatory cytokines (granzyme B, perforin B), and CAR downstream signaling molecules (pZAP70 and pS6) (Figure 5C). Differential protein expression between CD19-depleted CAT and FMC63 CAR T cells was only observed for pRB and CD69 (supplemental Figure 7F). Both CAT and FMC63 CAR T cells exhibited increased expression of activation and cytotoxic markers with respect to the UNTR controls that they were

Figure 3 (continued) cells (n = 6 HDs, n = 2 independent experiments) (right). (E) Bar plots showing the expression of mass cytometry EMD scores for CD25, HLA-DR, NFAT1, FOXP3, pZAP70, pS6, pp38, pCREB, pRB, and CD4 in stimulated CAR T cells at 24 hours upon stimulation. The data shown are normalized to stimulated $CD3^+$ UNTR T cells. The dotted horizontal line (0) represents the expression of a specific marker in stimulated $CD3^+$ UNTR T cells (n = 7 HDs, n = 2 independent experiments). (A-E) Bar plots show mean ± SEM. Each experimental condition is indicated by a specific color code (UNTR, gray; FMC63, blue; and CAT, red). Panels A-C,E show statistical significance calculated by paired *t* test; $^*P < .05$, $^{**}P < .01$, $^{***}P < .001$, and $^{****}P < .0001$. FDR, false discovery rate; MFI, mean fluorescent intensity; SEM, standard error of the mean.

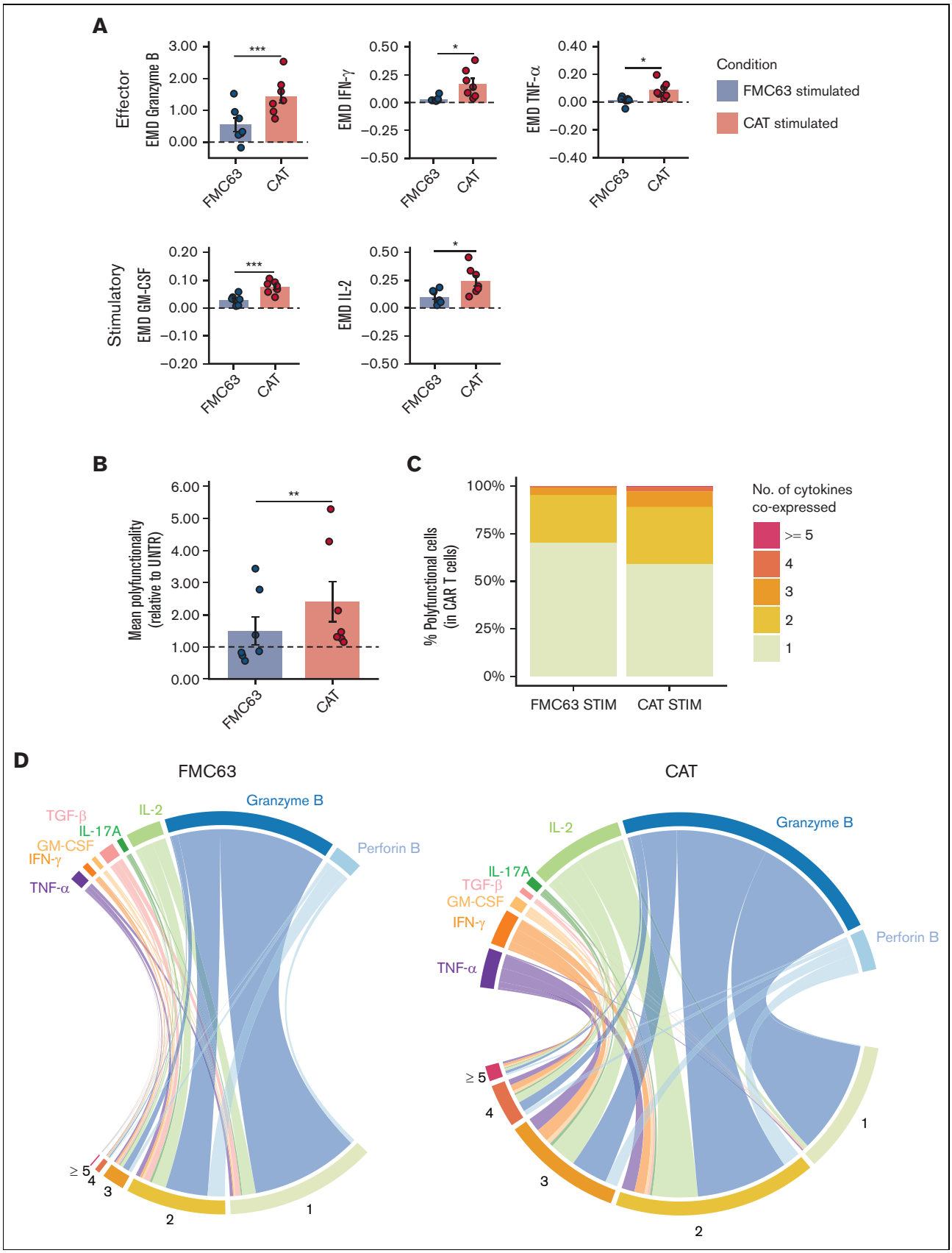

Figure 4.

normalized to, indicating similar levels of antigen-independent activation (Figure 5C).

When later exposed to NALM6, both CD19-depleted CAT and FMC63 were able to be activated, as shown by the upregulation of the expression of cytotoxic markers and cytokines compared with their unstimulated counterparts (supplemental Figures 10 and 11). No differences in the CD4:CD8 ratios or in the expression of exhaustion markers were observed between the 2 stimulated CAR conditions upon CD19 depletion (supplemental Figure 7G-H). Most importantly, upon antigenic stimulation, CD19-depleted CAT CAR T cells activated a molecular response with no statistically significant differences when compared with FMC63 (Figure 5D; supplemental Figure 7I), except for an increased expression of IL-2 (supplemental Figure 7I). The increased cytokine polyfunctionality observed in CAT vs FMC63 CAR T cells in standard manufacture condition (Figure 4) was no longer observed in CD19-depleted manufacture condition (Figure 5E).

Altogether these results demonstrate that residual B cells in the CAR T-cell manufacture can mediate an antigen-dependent activation priming, which is more pronounced in low-affinity CAT CAR T cells when compared with FMC63 CAR T cells. Such activation priming contributes to boosting CAT CAR T-cell response, because CAT CAR T cells generated from CD19-depleted PBMCs neither display increased activation priming nor exhibit increased molecular responses to antigenic stimulation with NALM6.

Discussion

Modulating CAR T-cell affinity may enable us to enhance antitumor response and long-term tumor surveillance, while minimizing CAR T-cell–related toxicity. We, thus, investigated the transcriptomic and proteomic phenotype of CD19 CAT CAR T cells, compared with the widely used FMC63, to begin unraveling the molecular mechanisms behind the observed preclinical and clinical differences between these 2 CD19 CARs.[11]

We found that CAT CARs induce stronger activation responses than FMC63, which could be explained by the faster target off-rate of low-affinity CARs. Faster dissociation requires fewer targets to serially trigger a larger number of CARs and amplify antitumoral response.[13] This would align with the proposed model of temporal and spatial summation of T-cell activation, in which signals from serially triggered immunoreceptors can be accumulated and integrated overtime to reach the threshold required for T-cell activation.[35] This model may also explain why low levels of residual donor B cells in the manufacture can induce stronger activation priming in CAT CAR T cells than in FMC63.

Our transcriptomic and protein profiling revealed that unstimulated CAT CAR T cells are functionally closer to antigen-activated CAR T cells than FMC63 CAR T cells, with a number of upregulated activation genes (*HLA-DBP1*, *HLA-DRA,* etc) and proteins (HLA-DR, CD25, and NFAT1). Despite these genes/proteins being commonly associated to T-cell activation, their basal expression is also increased in memory T cells as compared with T_{NAIVE} cells, as memory T cells are characterized by an open chromatin conformation favoring the access of transcription factors to immune response genes, thus ensuring a pool of readily available messenger RNAs that can be rapidly translated following stimulation.[36] This hypothesis is in agreement with the increased proportion of T_{CM} observed in CAT CAR T cells as compared with FMC63. However, further studies are needed to elucidate the molecular signaling underlying the preferential differentiation toward T_{CM} in low-affinity CAT CAR T cells.

By performing B-cell depletion before CAR T-cell manufacture, we have demonstrated that residual B cells in the CAR T-cell product are responsible for the activation priming observed in CAR T cells, which was more pronounced in CAT when compared with FMC63, and preferentially induce T_{CM} differentiation of CAT CAR T cells. This is consistent with the hypothesis that CAT serial triggering may amplify T-cell activation from lower antigen levels[13] and points to a boosting role of low-dose CD19-priming during CAR T-cell manufacture. The preferential T_{CM} phenotype in CAT CAR T cells might be owing to kinetic differences in clearance of residual B cells or to different downstream signaling after antigenic stimulation with low- vs high-affinity CAR T cells. Further work elucidating these mechanisms is needed. Recent results have shown that antigen-independent induction of CAR T-cell priming, by either 4-1BB-based tonic signaling[22] or by a low dose of hypomethylating agents,[23] can lead to enhanced CAR T antitumor functions in vivo and it is regulated by the recruitment of LCK or THEMIS-SHP1 phosphatase into the CAR synapse.[37] Our results indicate that low-dose antigen-specific priming can also promote CAR T-cell functionality in a CAR construct–specific manner with an enhanced effect in low-affinity CAR T cells.

When stimulated with CD19-expressing NALM6 cell line, CAT CAR T cells have a distinct transcriptomic and protein response to CD19 antigenic stimulation from FMC63 CAR T cells, with increased expression of proliferation, activation, and cytotoxic markers at both RNA and protein levels. In vivo clonal kinetics analyses have shown that single CD19 CAR T cells with higher expression of cytotoxic-related genes in the manufacture product, many of which are in common with ours (including *IFNG*, *HLA-DRA*, *CCL4*) and gave rise to superior in vivo expansion and survival, significantly contributing to later time points after adoptive transfer in patients.[19,38] Analysis of gene expression also revealed

Figure 4. Cytokine polyfunctionality in stimulated CAR-transduced T cells. (A) Bar plots showing the expression of mass cytometry EMD scores for effector (granzyme B, IFN-γ, TNF-α) and stimulatory (GM-CSF, IL-2) cytokines in stimulated CAR T cells. The data shown are normalized to stimulated $CD3^+$ UNTR T cells. The dotted horizontal line (0) represents the expression of a specific marker in stimulated $CD3^+$ UNTR T cells. (n = 7 HDs, n = 2 independent experiments). (B) Bar plots showing the mean cytokine polyfunctionality in stimulated CAR T cells, normalized to stimulated $CD3^+$ UNTR T cells. The dotted horizontal line (1) represents the mean polyfunctionality in stimulated $CD3^+$ UNTR T cells. (n = 7 HDs, n = 2 independent experiments). (C) Stacked bar plots showing the percentage of stimulated CAR T cells ($CD3^+mCherry^+$) expressing 1 to 4 or ≥5 cytokines per cell as measured by mass cytometry. (D) Circos plots showing all the combinations of the 8 cytokines in stimulated FMC63 (left) and CAT (right) CAR T cells analyzed by mass cytometry. The numbers indicate patterns of cytokine coexpression (from 1-4 or ≥5 cytokines/cell). A specific color code has been assigned to each cytokine. (A-B) Data represent mean ± SEM. Statistical significance was calculated by paired *t* test; $*P < .05$ and $***P < .001$. Each experimental condition is indicated by a specific color code (FMC63, blue and CAT, red). GM-CSF, granulocyte-macrophage colony-stimulating factor; SEM, standard error of the mean; TNF-α, tumor necrosis factor α.

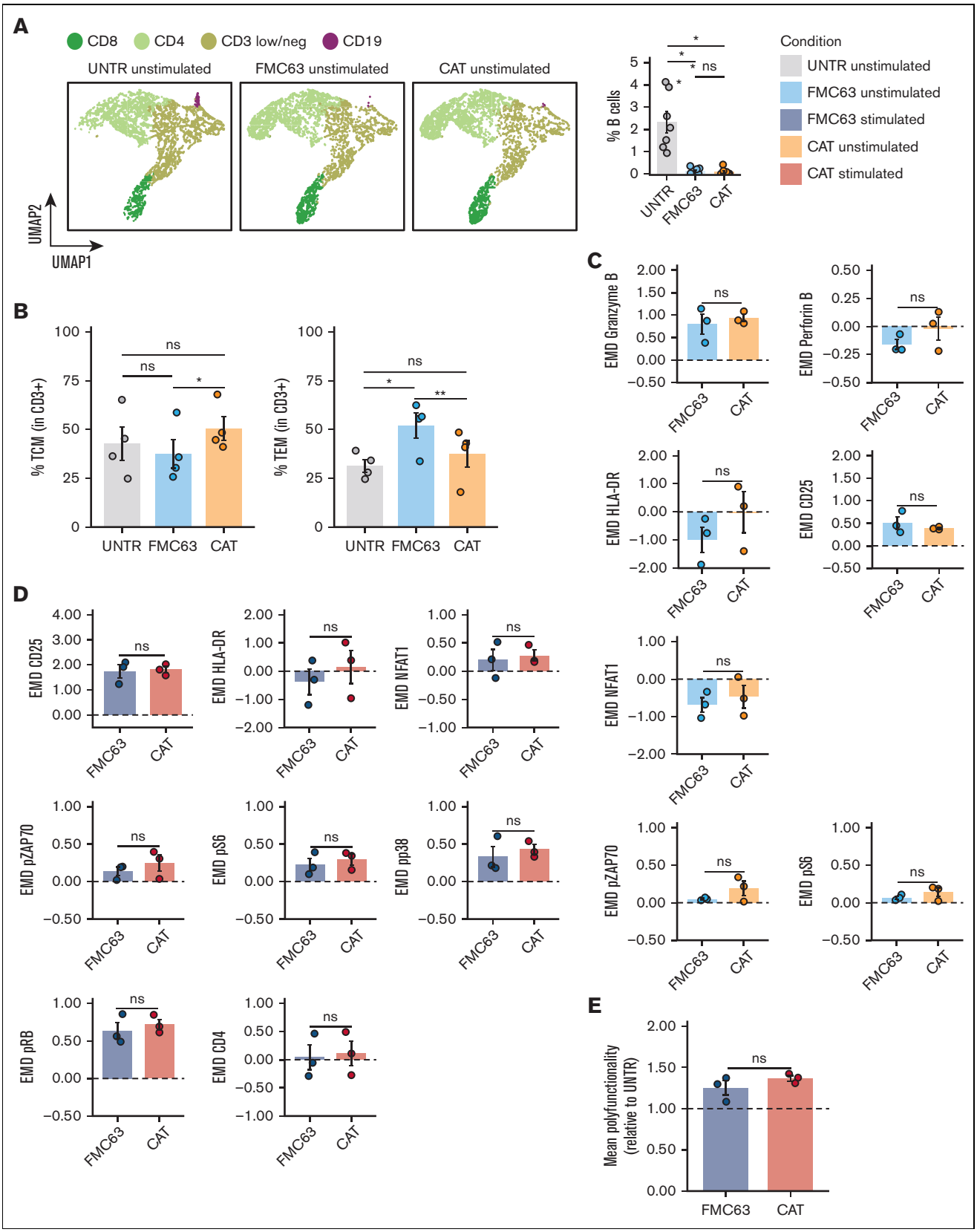

Figure 5. Molecular characterization of CAR T cells generated from CD19-depleted PBMCs. (A) UMAP representation of the 4 cell populations (CD8, CD4, CD3 low/neg, and CD19) identified by FlowSOM analysis in 4 representative unstimulated samples analyzed by mass cytometry at 24 hours poststimulation (left) (n = 4 HDs, n = 1

the upregulation of chemoattractive cytokines CCL4 and CCL3L1 in CAT, which induce T-cell homotypic interactions and promote the reciprocal exchange of self-reinforcing signals such as OX40L,[26,39] which are also upregulated in CAT. Single-cell transcriptomic studies have revealed that subsets of CAR T cells with elevated expression of CCL3 and CCL4 are associated with longer persistence in vivo[38] and achievement of complete remission.[40] Mass cytometry analyses revealed a CAT CAR T-cell enhanced activation protein profile, as measured by the increased expression of T-cell activation markers (CD25, HLA-DR) and CAR downstream signaling effectors (pZAP70, pp38, NFAT1, pCREB, FOXP3). Furthermore, CAT CAR T cells showed increased mTORC signaling (pS6 and pRB), which is commonly associated to cell proliferation and protein translation. Altogether, CAT CAR T cells' distinct gene expression and protein profiles are very much in line and likely responsible for the enhanced proliferative responses that CAT CAR T cells exhibited in vitro, in in vivo murine models, and in patients, as previously reported by Ghorashian et al.[11]

Upon stimulation, CAT CAR T cells were characterized by a unique polyfunctional pattern of cytokine expression, with a marked increase in the frequency of single CAR T cells expressing ≥3 cytokines when compared with FMC63. The CAT polyfunctional profile was dominated by combinations of effector cytokines, consistent with their potent antitumor activity. It has been suggested that the ability of CAR T cells to produce multiple cytokines in response to antigen exposure is associated with improved antitumor responses in vivo[31] and cytokine polyfunctionality has recently been proposed as a criteria to predict CAR T-cell potency.[33] The increased cytokine polyfunctionality observed in CAT CAR T cells contributes to explaining their increased cytotoxic potential previously observed in in vitro settings and in in vivo murine models.[11]

In conclusion, we describe the molecular mechanisms underlying the low-affinity CAT CAR T-cell functional phenotype. We provide evidence that the potent and long-term antitumor responses observed with low-affinity CAT CAR T cells[11] reflect a distinct pattern of both activation priming and cytokine polyfunctionality. We show that low-affinity CAT CAR T cells are preferentially primed by low concentration of CD19-expressing B cells present in the manufacture and such priming is instrumental to their higher cytotoxic response upon stimulation. Although our observations are limited to low-affinity CAR, future work extending this characterization to a panel of low-affinity CARs might reveal whether these findings are generalizable. In future work, we will focus on elucidating the mechanism by which residual B cells in the starting material induce differential effects on low- vs high-affinity CAR T cells and whether there is a dose-dependent relationship between residual $CD19^+$ B cells and CAR T-cell functionality. This will have important implications for CAR T-cell manufacturing protocols.

Overall, our work has important implications for the future design of versatile CAR T-cells manufacturing protocols, capable of boosting efficacy and long-term persistence.

Acknowledgments

The authors are grateful to the UCL ICH Flow Cytometry facility for support in cell sorting. The authors are grateful to Thomas Adejumo (Fluidigm) for valuable suggestions regarding mass cytometry and assistance with protocol design. The authors also thank Anne Marijn Kramer (Amsterdam UMC) for generating CD19 FMC63 and CAT CAR transfer vector plasmids with S.G., M.A.P., and P.J.A. The authors acknowledge the contribution of UCL Genomics Facility.

This work was supported by the National Institute for Health and Care Research GOSH BRC (NIHR GOSH BRC 17PA01); the views expressed are those of the author(s) and not necessarily those of the National Health Service, National Institute for Health and Care Research, or Department of Health. Part of this work was supported by the Leukaemia UK John Goldman Fellowship (A. Giustacchini) (2018/JGF/003), the Rosetrees Trust fund (A. Giustacchini) (M700), and the Academy of Medical Sciences Springboard Award (A. Giustacchini) (SBF004\1025).

Authorship

Contribution: I.M.M. designed, performed and analyzed experiments, performed bioinformatic analyses of mass cytometry experiments, and contributed to writing the manuscript; E.G.-C. performed bioinformatic analyses of transcriptomic data and wrote the relative bioinformatic supplemental information; R.V.C.P. performed experiments and bioinformatic analyses of mass cytometry and transcriptomic data; F.C.R. provided data analysis tools and contributed to bioinformatic analyses of mass cytometry experiments; P.P.C. performed transcriptomic bioinformatic analyses data checks and contributed to writing the bioinformatic supplemental information; J. S., M.S., S.W.W., A. Guvenel, and E.K. performed experiments; A.E. provided support to cell sorting; J.F. provided analytical pipelines and useful discussion for the

Figure 5 (continued) independent experiment). Cell types are indicated by different colors. Percentage of residual B cells detected by mass cytometry in unstimulated samples at 24 hours poststimulation (right) (n = 7 HDs, n = 2 independent experiments). (B) Bar plots showing the percentage of T_{CM} ($CD45RA^-CD62L^+$) (left) and T_{EM} ($CD45RA^-CD62L^-$) (right) in unstimulated CD19-depleted $CD3^+$ UNTR T cells and FMC63 and CAT CAR T cells measured by FACS (n = 4 HDs, n = 1 independent experiment). (C) Bar plots showing the expression of mass cytometry EMD scores for granzyme B, perforin B, HLA-DR, CD25, NFAT1, pZAP70, and pS6 in unstimulated CD19-depleted CAR T cells at 24 hours upon stimulation. The data shown are normalized to stimulated $CD3^+$ UNTR T cells. The dotted horizontal line (0) represents the expression of a specific marker in unstimulated $CD3^+$ CD19-depleted UNTR T cells. (n = 3 HDs, n = 1 independent experiment). (D) Bar plots showing the expression of mass cytometry EMD scores for CD25, HLA-DR, NFAT1, pZAP70, pS6, pp38, pRB, and CD4 in stimulated CD19-depleted CAR T cells at 24 hours upon stimulation. The data shown are normalized to stimulated $CD3^+$ UNTR T cells. The dotted horizontal line (0) represents the expression of a specific marker in stimulated CD19-depleted $CD3^+$ UNTR T cells (n = 3 HDs, n = 1 independent experiment). (E) Bar plots showing the mean polyfunctionality in CD19-depleted CAR T cells at 24 hours upon stimulation. The data shown are normalized to stimulated $CD3^+$ UNTR T cells. The dotted horizontal line (1) represents the mean polyfunctionality in stimulated $CD3^+$ CD19-depleted UNTR T cells (n = 3 HDs, n = 1 independent experiment). (A-E) Each experimental condition is indicated by a specific color code (unstimulated conditions: UNTR, light gray; FMC63, light blue; CAT, orange; stimulated conditions: FMC63, blue; CAT, red). Bar plots show mean ± SEM. Statistical significance was calculated by paired *t* test; $*P < .05$ and $**P < .01$. SEM, standard error of the mean.

analysis and normalization of mass cytometry data; S.G. and M.P. provided CAR constructs; C.J.T. provided expertise in mass cytometry and reagents; P.J.A. provided reagents and expertise and contributed to writing the manuscript; S.C. supervised the bioinformatic analyses and contributed to writing the manuscript; A. Giustacchini designed and supervised the project, performed and analyzed experiments, and wrote the manuscript; and all authors provided critical feedback and helped shape the research, analyses, and manuscript.

Conflict-of-interest disclosure: S.G. received speaker's honoraria from Novartis and patents and royalties from UCLB. M.A.P. owns stock in and is in part employed by Autolus Therapeutics, that has licensed CAT CAR. P.J.A. has received royalties for a patent related to CAT CAR from Autolus and receives research funding from Autolus. The remaining authors declare no competing financial interests.

ORCID profiles: I.M.M., 0000-0002-3550-2129; E.G.-C., 0000-0002-7355-2960; F.C.R., 0000-0002-1376-1242; J.S., 0000-0002-4563-5531; P.P.C., 0000-0002-8687-4942; E.K., 0000-0003-3368-7331; J.F., 0000-0003-3302-2241; S.G., 0000-0002-1555-2946; M.A.P., 0000-0002-8347-9867; C.J.T., 0000-0003-4712-2737; S.C., 0000-0002-5819-4210; P.J.A., 0000-0003-0480-3911; A.G., 0000-0002-8733-8594.

Correspondence: Alice Giustacchini, Zayed Centre for Research into Rare Disease in Children, UCL Great Ormond Street Institute of Child Health, 20 Guilford St, London WC1N 1DZ, United Kingdom; email: a.giustacchini@ucl.ac.uk.

References

1. Miliotou AN, Papadopoulou LC. CAR T-cell therapy: a new era in cancer immunotherapy. *Curr Pharm Biotechnol*. 2018;19(1):5-18.
2. Pehlivan KC, Duncan BB, Lee DW. CAR-T cell therapy for acute lymphoblastic leukemia: transforming the treatment of relapsed and refractory disease. *Curr Hematol Malig Rep*. 2018;13(5):396-406.
3. Lee DW, Gardner R, Porter DL, et al. Current concepts in the diagnosis and management of cytokine release syndrome. *Blood*. 2014;124(2):188-195.
4. Gust J, Hay KA, Hanafi LA, et al. Endothelial activation and blood-brain barrier disruption in neurotoxicity after adoptive immunotherapy with CD19 CAR-T cells. *Cancer Discov*. 2017;7(12):1404-1419.
5. Watanabe K, Kuramitsu S, Posey AD Jr, June CH. Expanding the therapeutic window for CAR T cell therapy in solid tumors: the knowns and unknowns of CAR T cell biology. *Front Immunol*. 2018;9:2486.
6. Kowolik CM, Topp MS, Gonzalez S, et al. CD28 costimulation provided through a CD19-specific chimeric antigen receptor enhances in vivo persistence and antitumor efficacy of adoptively transferred T cells. *Cancer Res*. 2006;66(22):10995-11004.
7. Singh AP, Zheng X, Lin-Schmidt X, et al. Development of a quantitative relationship between CAR-affinity, antigen abundance, tumor cell depletion and CAR-T cell expansion using a multiscale systems PK-PD model. *MAbs*. 2020;12(1):1688616.
8. Chmielewski M, Hombach A, Heuser C, Adams GP, Abken H. T cell activation by antibody-like immunoreceptors: increase in affinity of the single-chain fragment domain above threshold does not increase T cell activation against antigen-positive target cells but decreases selectivity. *J Immunol*. 2004;173(12):7647-7653.
9. Caruso HG, Hurton LV, Najjar A, et al. Tuning sensitivity of CAR to EGFR density limits recognition of normal tissue while maintaining potent antitumor activity. *Cancer Res*. 2015;75(17):3505-3518.
10. Liu X, Jiang S, Fang C, et al. Affinity-tuned ErbB2 or EGFR chimeric antigen receptor T cells exhibit an increased therapeutic index against tumors in mice. *Cancer Res*. 2015;75(17):3596-3607.
11. Ghorashian S, Kramer AM, Onuoha S, et al. Enhanced CAR T cell expansion and prolonged persistence in pediatric patients with ALL treated with a low-affinity CD19 CAR. *Nat Med*. 2019;25(9):1408-1414.
12. Roddie C, Dias J, O'Reilly MA, et al. Durable responses and low toxicity after fast off-rate CD19 chimeric antigen receptor-T therapy in adults with relapsed or refractory B-cell acute lymphoblastic leukemia. *J Clin Oncol*. 2021;39(30):3352-3363.
13. Valitutti S, Muller S, Cella M, Padovan E, Lanzavecchia A. Serial triggering of many T-cell receptors by a few peptide-MHC complexes. *Nature*. 1995;375(6527):148-151.
14. Michelozzi IM, Sufi J, Adejumo TA, Amrolia PJ, Tape CJ, Giustacchini A. High-dimensional functional phenotyping of preclinical human CAR T cells using mass cytometry. *STAR Protoc*. 2022;3(1):101174.
15. Wang X, Popplewell LL, Wagner JR, et al. Phase 1 studies of central memory-derived CD19 CAR T-cell therapy following autologous HSCT in patients with B-cell NHL. *Blood*. 2016;127(24):2980-2990.
16. Wang X, Wong CW, Urak R, et al. Comparison of naive and central memory derived CD8(+) effector cell engraftment fitness and function following adoptive transfer. *Oncoimmunology*. 2016;5(1):e1072671.
17. Orlova DY, Zimmerman N, Meehan S, et al. Earth mover's distance (EMD): a true metric for comparing biomarker expression levels in cell populations. *PLoS One*. 2016;11(3):e0151859.
18. Kaufman L, Rousseeuw PJ. Fuzzy analysis (program FANNY). In: *Finding Groups in Data: An Introduction to Cluster Analysis*. Wiley; 1990:164-198.
19. Gomes-Silva D, Mukherjee M, Srinivasan M, et al. Tonic 4-1BB costimulation in chimeric antigen receptors impedes T cell survival and is vector-dependent. *Cell Rep*. 2017;21(1):17-26.

20. Frigault MJ, Lee J, Basil MC, et al. Identification of chimeric antigen receptors that mediate constitutive or inducible proliferation of T cells. *Cancer Immunol Res*. 2015;3(4):356-367.
21. Long AH, Haso WM, Shern JF, et al. 4-1BB costimulation ameliorates T cell exhaustion induced by tonic signaling of chimeric antigen receptors. *Nat Med*. 2015;21(6):581-590.
22. Singh N, Frey NV, Engels B, et al. Antigen-independent activation enhances the efficacy of 4-1BB-costimulated CD22 CAR T cells. *Nat Med*. 2021; 27(5):842-850.
23. Wang Y, Tong C, Dai H, et al. Low-dose decitabine priming endows CAR T cells with enhanced and persistent antitumour potential via epigenetic reprogramming. *Nat Commun*. 2021;12(1):409.
24. Allan SE, Crome SQ, Crellin NK, et al. Activation-induced FOXP3 in human T effector cells does not suppress proliferation or cytokine production. *Int Immunol*. 2007;19(4):345-354.
25. Ran Q, Hao P, Xiao Y, et al. CRIF1 interacting with CDK2 regulates bone marrow microenvironment-induced G0/G1 arrest of leukemia cells. *PLoS One*. 2014;9(2):e85328.
26. Soroosh P, Ine S, Sugamura K, Ishii N. OX40-OX40 ligand interaction through T cell-T cell contact contributes to CD4 T cell longevity. *J Immunol*. 2006;176(10):5975-5987.
27. Holling TM, van der Stoep N, Quinten E, van den Elsen PJ. Activated human T cells accomplish MHC class II expression through T cell-specific occupation of class II transactivator promoter III. *J Immunol*. 2002;168(2):763-770.
28. Gourley TS, Chang CH. Cutting edge: the class II transactivator prevents activation-induced cell death by inhibiting Fas ligand gene expression. *J Immunol*. 2001;166(5):2917-2921.
29. Betts MR, Nason MC, West SM, et al. HIV nonprogressors preferentially maintain highly functional HIV-specific CD8+ T cells. *Blood*. 2006;107(12): 4781-4789.
30. Caccamo N, Guggino G, Joosten SA, et al. Multifunctional CD4(+) T cells correlate with active Mycobacterium tuberculosis infection. *Eur J Immunol*. 2010;40(8):2211-2220.
31. Rossi J, Paczkowski P, Shen YW, et al. Preinfusion polyfunctional anti-CD19 chimeric antigen receptor T cells are associated with clinical outcomes in NHL. *Blood*. 2018;132(8):804-814.
32. Xhangolli I, Dura B, Lee G, Kim D, Xiao Y, Fan R. Single-cell analysis of CAR-T cell activation reveals a mixed TH1/TH2 response independent of differentiation. *Genomics Proteomics Bioinformatics*. 2019;17(2):129-139.
33. Spiegel JY, Patel S, Muffly L, et al. CAR T cells with dual targeting of CD19 and CD22 in adult patients with recurrent or refractory B cell malignancies: a phase 1 trial. *Nat Med*. 2021;27(8):1419-1431.
34. Van Gassen S, Callebaut B, Van Helden MJ, et al. FlowSOM: using self-organizing maps for visualization and interpretation of cytometry data. *Cytometry A*. 2015;87(7):636-645.
35. Rachmilewitz J, Lanzavecchia A. A temporal and spatial summation model for T-cell activation: signal integration and antigen decoding. *Trends Immunol*. 2002;23(12):592-595.
36. Weng NP, Araki Y, Subedi K. The molecular basis of the memory T cell response: differential gene expression and its epigenetic regulation. *Nat Rev Immunol*. 2012;12(4):306-315.
37. Sun C, Shou P, Du H, et al. THEMIS-SHP1 recruitment by 4-1BB tunes LCK-mediated priming of chimeric antigen receptor-redirected T cells. *Cancer Cell*. 2020;37(2):216-225.e216.
38. Sheih A, Voillet V, Hanafi LA, et al. Clonal kinetics and single-cell transcriptional profiling of CAR-T cells in patients undergoing CD19 CAR-T immunotherapy. *Nat Commun*. 2020;11(1):219.
39. Castellino F, Huang AY, Altan-Bonnet G, Stoll S, Scheinecker C, Germain RN. Chemokines enhance immunity by guiding naive CD8+ T cells to sites of CD4+ T cell-dendritic cell interaction. *Nature*. 2006;440(7086):890-895.
40. Bai Z, Lundh S, Kim D, et al. Single-cell multiomics dissection of basal and antigen-specific activation states of CD19-targeted CAR T cells. *J Immunother Cancer*. 2021;9(5):e002328.